Journal of Solid State Electrochemistry (2024) 28:2093–2101
https://doi.org/10.1007/s10008-023-05722-4

ORIGINAL PAPER

$NaSn_{0.02}Ti_{1.98}(PO_4)_3$/C as a promising anode material with high performance for sodium-ion batteries

Jiajie Gu[1] · Shaojie Zhang[1] · Xinyue Zhang[1] · Chuanyang Li[1] · Aohua Wu[1] · Qiaohui Li[1] · Wutao Mao[1] · Keyan Bao[1]

Received: 30 August 2023 / Revised: 18 October 2023 / Accepted: 20 October 2023 / Published online: 10 November 2023
© The Author(s), under exclusive licence to Springer-Verlag GmbH Germany, part of Springer Nature 2023

Abstract
In this paper, $NaSn_{0.02}Ti_{1.98}(PO_4)_3$/C composite material was prepared by spray drying method combined with high-temperature calcination, which can improve the electrochemical performance of $NaTi_2(PO_4)_3$. The doping of Sn^{4+} increases the lattice spacing of $NaTi_2(PO_4)_3$, thereby accelerating the diffusion coefficient of Na^+. The carbon doped on $NaTi_2(PO_4)_3$ reduces the charge transfer impedance and enhances the ion diffusion coefficient. As a result, $NaSn_{0.02}Ti_{1.98}(PO_4)_3$/C exhibits improved electrochemical performance. The specific capacity for the initial discharge of $NaSn_{0.02}Ti_{1.98}(PO_4)_3$/C at 1C, 5C, 10C and 20C rates are 108 mAh/g, 86 mAh/g, 76.3 mAh/g, and 71.4 mAh/g, respectively. After 1400 cycles at 10C, the capacity of the material decreases to 64.3 mAh/g, with a capacity retention rate of 84.2%. Therefore, $NaSn_{0.02}Ti_{1.98}(PO_4)_3$/C exhibits fast charge/discharge performance as well as cycling stability.

Keywords Electrochemical performance · $NaTi_2(PO_4)_3$ · Sn-doped · Carbon-doped · Fast charge/discharge performance

Introduction

In recent years, with the rapid development of modern portable electronics, new energy vehicles, and grid energy storage, the demand for advanced battery energy storage systems with high energy density has increased dramatically [1–3]. Because of their plentiful reserves and low cost, sodium-ion batteries (SIBs) have gained a lot of attention and offer a lot of potential as a form of renewable energy storage [4–7]. SIB materials possess characteristics such as high capacity and high safety performance. Currently, the research on negative electrode materials for SIBs mainly focuses on carbon materials [8], metal selenides [9], metal sulfides [10], and phosphate compounds [11]. Among these materials, phosphate-based compounds with Na as the main constituent are the optimal choice as negative electrode materials. This is due to their strong P–O covalent bonding, which offers superior thermal and structural stabilities. Among these phosphate-based materials, $NaTi_2(PO_4)_3$ with the NASICON structure has been gaining increasing attention owing to its vast theoretical potential (133 mAh/g), inexpensive cost, and good safety performance. It is considered a promising negative electrode material [12–15].

$NaTi_2(PO_4)_3$ exhibits thermal stability and a high theoretical capacity, but its slow charge transfer kinetics and low electronic conductivity result in low-capacity retention and poor rate performance [16–18]. Attempts have been made to enhance the electrochemical performance of $NaTi_2(PO_4)_3$ through carbon coating [16, 19], element doping [15, 20], or synergistic effects of carbon and element doping [5, 14, 17, 21–24]. For example, Mg-doped and carbon-doped $NaTi_2(PO_4)_3$ [25, 26], Mn-doped and carbon-doped $NaTi_2(PO_4)_3$ [23], Al-doped and carbon-doped $NaTi_2(PO_4)_3$ [14], Zr-doped and carbon-doped $NaTi_2(PO_4)_3$ [22], Fe-doped and carbon-doped $NaTi_2(PO_4)_3$ [27], and Cr-doped and carbon-doped $NaTi_2(PO_4)_3$ [28] have been reported. He prepared Zr-doped and carbon-coated $NaTi_2(PO_4)_3$ [22], which improved the electrochemical performance of $NaTi_2(PO_4)_3$, and was applied to aqueous LIBs. The capacity of discharge of $NaTi_{1.9}Zr_{0.1}(PO_4)_3$/C at 0.2C, 3C, and 15C were 112.5 mAh/g, 102.7 mAh/g, and 94.1 mAh/g, respectively. Wu prepared Al-doped and carbon-coated $NaTi_2(PO_4)_3$ for aqueous SIBs [14], showing 102.9 mAh/g initial discharge capacity and 90.1 mAh/g reversible capacity after 200 cycles at 10C.

✉ Wutao Mao
maowutao@126.com

✉ Keyan Bao
baokeyan@126.com

[1] Resource Environment & Clean Energy Laboratory, School of Chemical and Environmental Engineering, Jiangsu University of Technology, Changzhou 213001, China

Zhao studied the improvement of electrochemical capability of $NaTi_2(PO_4)_3$ by Mg doping and carbon coating [26] and applied it to organic SIBs. The specific capacity of the material was 94.4 mAh/g at a current density of 5 A/g. After 300 cycles, the rate of capacity retention reached 99.1%, showing good cycle stability. Qu studied the improvement of Mn doping and carbon coating on the electrochemical performance of $NaTi_2(PO_4)_3$ [23], which was applied to organic SIBs. It showed 116 mAh/g at 1C and 92 mAh/g after 1000 cycles at 20C (88% capacity retention).

After conducting research, it has been found that only a few researchers have utilized Sn-doped $NaTi_2(PO_4)_3$. The low cost of tin as a dopant makes it favorable for industrial applications. In this study, we prepared $NaSn_{0.02}Ti_{1.98}(PO_4)_3/C$ and applied it in organic SIBs. The electrochemical performance of the material was systematically investigated. The results indicate that the doping of Sn and carbon significantly improved performance of $NaTi_2(PO_4)_3$ electrochemically.

Experimental

Material synthesis

Firstly, 2.5 mmol of $C_6H_5Na_3O_7$ (0.645 g), 14.7 mmol of $C_8H_{20}O_4Ti$ (3.35 g), 0.3 mmol of $C_4H_{10}O_2Sn$ (0.063 g), and 22.5 mmol of $NH_4H_2PO_4$ (2.59 g) are added to a ball mill containing 40 g of water. The mixture is then ball-milled for 5 h at a constant temperature of 20 °C and a rotation speed of 500 rpm. After ball milling, adjust the inlet temperature of the spray dryer to 220 °C and the outlet temperature to around 80 °C. Once the conditions are met, start the feeding process with a peristaltic pump operating at a rate of 20 rpm to obtain the precursor. The dried solid powder was placed in a corundum crucible and heated at 900 °C for 10 h in an N_2 atmosphere at a rate of 5 °C/min to obtain the $NaSn_{0.02}Ti_{1.98}(PO_4)_3/C$. The $NaTi_2(PO_4)_3/C$ was obtained by removing the tin source $C_4H_{10}O_2Sn$, while other experimental conditions remained unchanged. The $NaTi_2(PO_4)_3$ was obtained by removing the tin source $C_4H_{10}O_2Sn$ and replacing $C_6H_5Na_3O_7$ with Na_2CO_3, while other experimental conditions remained unchanged.

Characterizations

X-ray diffractometer (X'Pert Powder XRD) analysis was performed to determine the purity of the produced material. A thermogravimetric analyzer (STA25000 TG) was used, and mass loss was recorded to quantify the carbon content of the material. Micromorphology of different composites observed by scanning electron microscope (S-3400N SEM) and EDS analyzed the distribution of elements in the composites. Inductively coupled plasma atomic emission spectrometry was utilized to measure the Sn content using the Thermo ICP6300 ICP-AES..

Electrode preparation and electrochemical testing

The working electrode consisting of 70% active material, 20% acetylene black, and 10% sodium carboxymethyl cellulose (adhesive) was prepared by placing these materials in a 50 ml agate spherule tank with N-methylpyrrolidone (NMP), ball milling for 1 h. The mixture is applied to the copper foil. After vacuum drying at 110 ℃ for 12 h, the electrode material was cut into small circles with an area of 1.13 cm^2, where the mass load of the electrode was about 1 mg/cm^2. A CR2032-type coin cell was assembled in an argon-filled glove box with water and oxygen concentrations of less than 0.1 ppm. The battery is mainly composed of working electrode (prepared electrode), electrode level (sodium metal sheet), diaphragm (glass fiber), and electrolyte (1 M $NaClO_4$ dissolved in a mixture solution of ethyl carbonate and dimethyl carbonate (volume ratio, 1:1)). Constant current/charge test was conducted using Land-2001A. An electrochemical workstation (CHI660E) was used for cyclic voltammetry (CV) measurements and EIS investigations. Constant discharge/charge test and CV test voltage range are consistent; both are 1.5–3 V. The range of EIS frequency is 200 kHz to 10 MHz.

Results and discussion

Figure 1a is the XRD of $NaTi_2(PO_4)_3/C$ and $NaSn_{0.02}Ti_{1.98}(PO_4)_3/C$. The results indicate that all sharp diffraction peaks of the two samples correspond to the $NaTi_2(PO_4)_3$ standard card (PDF#84-2009). In the patterns, there were no impurity peaks to be seen. Figure 1b shows the magnification of diffraction peaks (104), (110), (113), and (202) of $NaTi_2(PO_4)_3/C$ and $NaSn_{0.02}Ti_{1.98}(PO_4)_3/C$ in the range of 20 to 30°. Figure 1c shows the magnification of diffraction peaks (116) and (300) of $NaTi_2(PO_4)_3/C$ and $NaSn_{0.02}Ti_{1.98}(PO_4)_3/C$ in the range of 30 to 40°. It can be observed that the diffraction peaks of $NaSn_{0.02}Ti_{1.98}(PO_4)_3/C$ have shifted to the left, indicating a decrease in angle. According to Bragg formula, the diffraction peak position of the $NaSn_{0.02}Ti_{1.98}(PO_4)_3/C$ shifts to a smaller angle, indicating that the lattice expansion and the ion diffusion channel becoming wider, consistent with previously reported results [14, 29, 30]. The doping of Sn^{4+} can increase the lattice spacing of $NaTi_2(PO_4)_3$, and the ionic radius of Sn^{4+} (69 pm) is larger than that of Ti^{4+} (60.5 pm). Increasing the cell size will widen the transfer path of Na^+ within the crystal structure, thereby accelerating the diffusion coefficient of Na^+. The crystal cell parameters of $NaTi_2(PO_4)_3$ and $NaSn_{0.02}Ti_{1.98}(PO_4)_3/C$ were obtained after refining the XRD data using Rietveld (Fig. 1e, f). It can be seen from Table 1 that for $NaSn_{0.02}Ti_{1.98}(PO_4)_3/C$, the lattice parameter

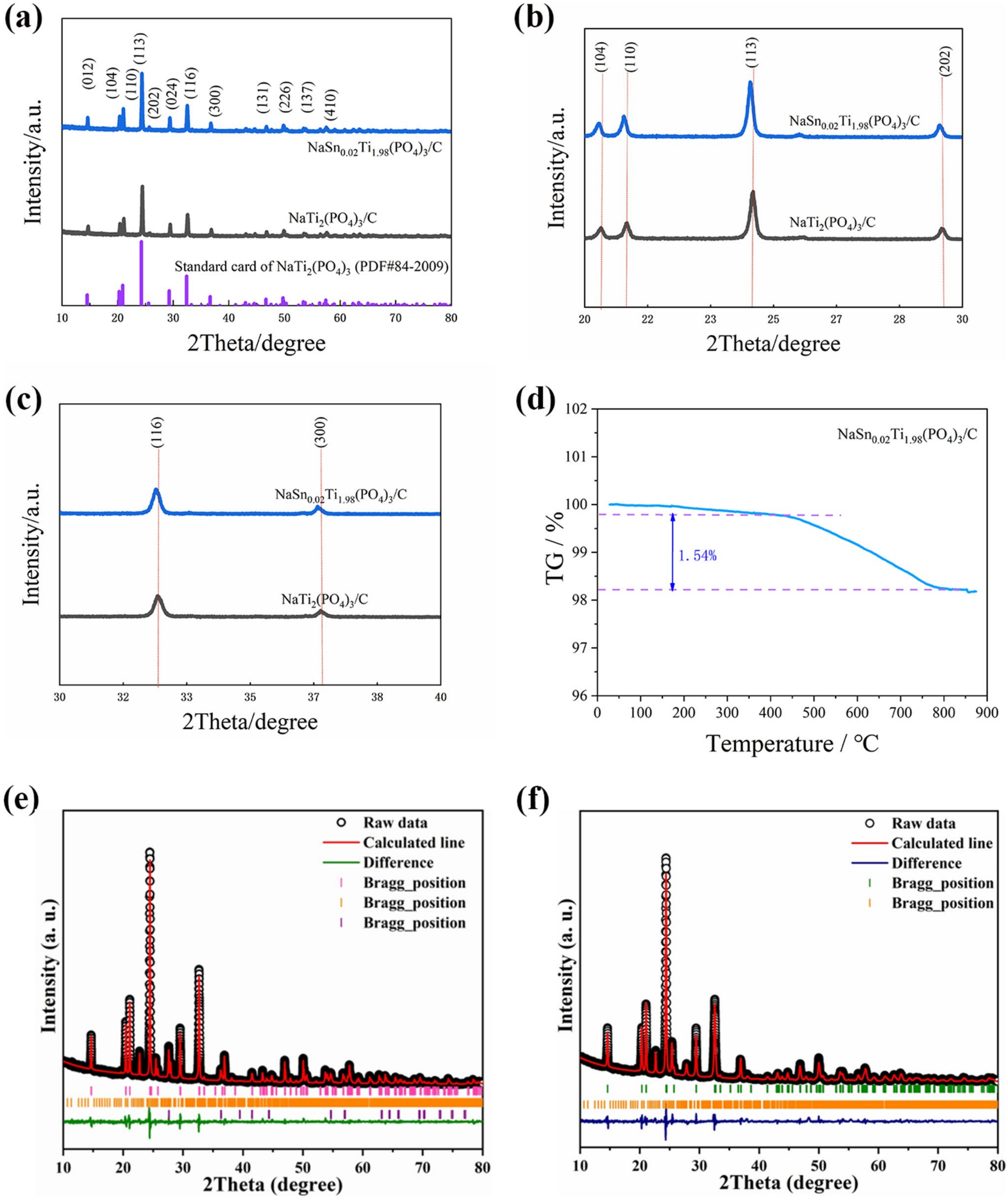

Fig. 1 **a** XRD of $NaTi_2(PO_4)_3$/C and $NaSn_{0.02}Ti_{1.98}(PO_4)_3$/C, **b** amplification of diffraction peaks (104), (110), (113), and (202) of $NaTi_2(PO_4)_3$/C and $NaSn_{0.02}Ti_{1.98}(PO_4)_3$/C, **c** amplification of diffraction peaks (116) and (300) of $NaTi_2(PO_4)_3$/C and $NaSn_{0.02}Ti_{1.98}(PO_4)_3$/C, **d** TGA of $NaSn_{0.02}Ti_{1.98}(PO_4)_3$/C, **e** refined XRD of $NaTi_2(PO_4)_3$, **f** refined XRD of $NaSn_{0.02}Ti_{1.98}(PO_4)_3$/C

Table 1 Lattice parameters and R factor of $NaTi_2(PO_4)_3$, $NaSn_{0.02}Ti_{1.98}(PO_4)_3/C$

Phase name	a (Å)	b (Å)	c (Å)	R_{wp}	R_p	Chi^2
$NaTi_2(PO_4)_3$	8.447119	8.447119	21.692232	8.26%	6.14%	0.4
$NaSn_{0.02}Ti_{1.98}(PO_4)_3/C$	8.433171	8.433171	21.779633	7.76%	5.29%	0.73

c = 21.7796 Å which is an increases of 0.40% compared to $NaTi_2(PO_4)_3$. The unit cell volume of $NaTi_2(PO_4)_3$ is 1340.5 Å^3, and the unit cell volume of $NaSn_{0.02}Ti_{1.98}(PO_4)_3/C$ is 1341.4 Å^3, which is 0.06% larger than that of $NaTi_2(PO_4)_3$. And expanded cell will result in larger sodium ion diffusion channel.

The TG test results (Fig. 1d) show that the weight decreases in the temperature range of 450–750 °C, which is due to the reaction and pyrolysis of carbon in sodium citrate in the material with air (it has been studied that the tin source will not decompose within 750 °C). Doping a small amount of carbon in the material can improve the electronic conductivity of the material, thereby enhancing the electrode material's performance. According to the curve in Fig. 1d, the carbon content in the $NaSn_{0.02}Ti_{1.98}(PO_4)_3/C$ sample is about 1.54%.

Figure 2a–d are the SEM images of $NaTi_2(PO_4)_3/C$ and $NaSn_{0.02}Ti_{1.98}(PO_4)_3/C$, respectively. From Fig. 2a, c, it can be seen that both $NaTi_2(PO_4)_3/C$ and $NaSn_{0.02}Ti_{1.98}(PO_4)_3/C$ are microspheres, and the distribution of microspheres is relatively uniform, without great difference. The magnified images in Fig. 2b, d show $NaTi_2(PO_4)_3/C$ particles and $NaSn_{0.02}Ti_{1.98}(PO_4)_3/C$ particles, respectively. It is evident that the micro-sized particles of both materials are composed of smaller particles, having a particle size distribution that ranges from 1 to 3 μm. In addition, the EDS mapping of C, O, Ti, P, Na, and Sn are shown in Fig. 2e for $NaSn_{0.02}Ti_{1.98}(PO_4)_3/C$. Sn and C are equally distributed and successfully doped in the $NaSn_{0.02}Ti_{1.98}(PO_4)_3/C$ sample, as evidenced by the fact that the distribution of Sn and C are consistent with the distribution of O, Ti, P, and Na. The content of Sn in the sample was measured by ICP. The mass percentage of Sn element in $NaSn_{0.02}Ti_{1.98}(PO_4)_3/C$ is about 1.42%.

We characterized its electrochemical performance. From Fig. 3a, it can be observed that at 1C, the initial overpotential of $NaTi_2(PO_4)_3/C$ is 252.6 mV. At 2C, 5C, 10C, and 20C, the potential differences are 389 mV, 718.9 mV, 719 mV, and 994.4 mV, respectively. The capacities at 1C, 2C, 5C, 10C, and 20C are 100.4 mAh/g, 91.6 mAh/g, 76.9 mAh/g, 65.8 mAh/g, and 55.8 mAh/g, respectively. From Fig. 3b, it can be observed that at 1C, the initial overpotential of $NaSn_{0.02}Ti_{1.98}(PO_4)_3/C$ is 185.3 mV. At 2C, 5C, 10C, and 20C, the potential differences are 317.5 mV, 531.7 mV, 598.9 mV, and 789.6 mV, respectively. The capacities at 1C, 2C, 5C, 10C, and 20C are 108 mAh/g, 102.3 mAh/g, 91.6 mAh/g, 78.4 mAh/g, and 71.4 mAh/g, respectively. It can be seen that the overpotential of $NaSn_{0.02}Ti_{1.98}(PO_4)_3/C$ becomes smaller and the capacity becomes larger. To further investigate the electrochemical performance of the material, we conducted rate performance tests (Fig. 3c, d), which clearly show the material's ability for rapid charge and discharge. As shown in Fig. 3d, the initial discharge-specific capacities of $NaSn_{0.02}Ti_{1.98}(PO_4)_3/C$ at 1C, 5C, 10C, and 20C are 108mAh/g, 86mAh/g, 76.3mAh/g, and 71.4mAh/g, respectively, all higher than those of $NaTi_2(PO_4)_3/C$ (Fig. 3c). Figure 3e is the cycling performance of $NaTi_2(PO_4)_3/C$ and $NaSn_{0.02}Ti_{1.98}(PO_4)_3/C$ at 10C. The initial discharge-specific capacity of $NaTi_2(PO_4)_3/C$ is 79.9 mAh/g, which decays to 49.5 mAh/g after 1400 cycles, and the capacity retention rate is 61.9%. The initial discharge-specific capacity of $NaSn_{0.02}Ti_{1.98}(PO_4)_3/C$ is 76.3 mAh/g, which decays to 64.3 mAh/g after 1400 cycles, and the capacity retention rate is 84.2%. It has good fast charge-discharge performance and cycle stability.

Figure 4a–c is the CV curves of working electrode $NaTi_2(PO_4)_3$, $NaTi_2(PO_4)_3/C$, and $NaSn_{0.02}Ti_{1.98}(PO_4)_3/C$ in the voltage range of 1.5 ~ 3.0 V and the scan rate of 0.1 mV/s. In Fig. 4a, $NaTi_2(PO_4)_3$ shows two significant redox peaks at about 2.23 V/1.92 V, and the potential interval is about 340 mV. In Fig. 4b, $NaTi_2(PO_4)_3/C$ shows two significant redox peaks at about 2.23 V/2.05 V, with potential intervals of about 253 mV. In Fig. 4c, $NaSn_{0.02}Ti_{1.98}(PO_4)_3/C$ shows two significant redox peaks at about 2.23 V/2.05 V, with potential intervals of about 185 mV. In the CV curve, the ΔE between the peak potential difference of the cathode and anode reflects the polarization and dynamic characteristics of the electrodes. As is well known, the electron conduction resistance and ion diffusion resistance from materials are the main reason for polarization. Compared to $NaTi_2(PO_4)_3$, $NaTi_2(PO_4)_3/C$ increases the electronic conductivity of the material due to carbon coating, which can effectively reduce the polarization of the electrode, thus exhibiting a smaller ΔE. Furthermore, $NaSn_{0.02}Ti_{1.98}(PO_4)_3/C$ exhibits a smaller ΔE than $NaTi_2(PO_4)_3/C$, indicating that $NaSn_{0.02}Ti_{1.98}(PO_4)_3/C$ has a smaller polarization, which is mainly attributed to the increase in Na^+ expansion coefficient caused by Sn^{4+} doping. Having the minimum polarization gives $NaSn_{0.02}Ti_{1.98}(PO_4)_3/C$ the best rate performance.

Electrical conductivity and Na^+ diffusion are widely regarded as the primary determining factors for electrode performance. Electrochemical impedance spectroscopy (EIS) measurements were conducted to elucidate the kinetic processes of the $NaTi_2(PO_4)_3$ electrode (Fig. 4d). As shown in Fig. 4d, the charge transfer resistance of

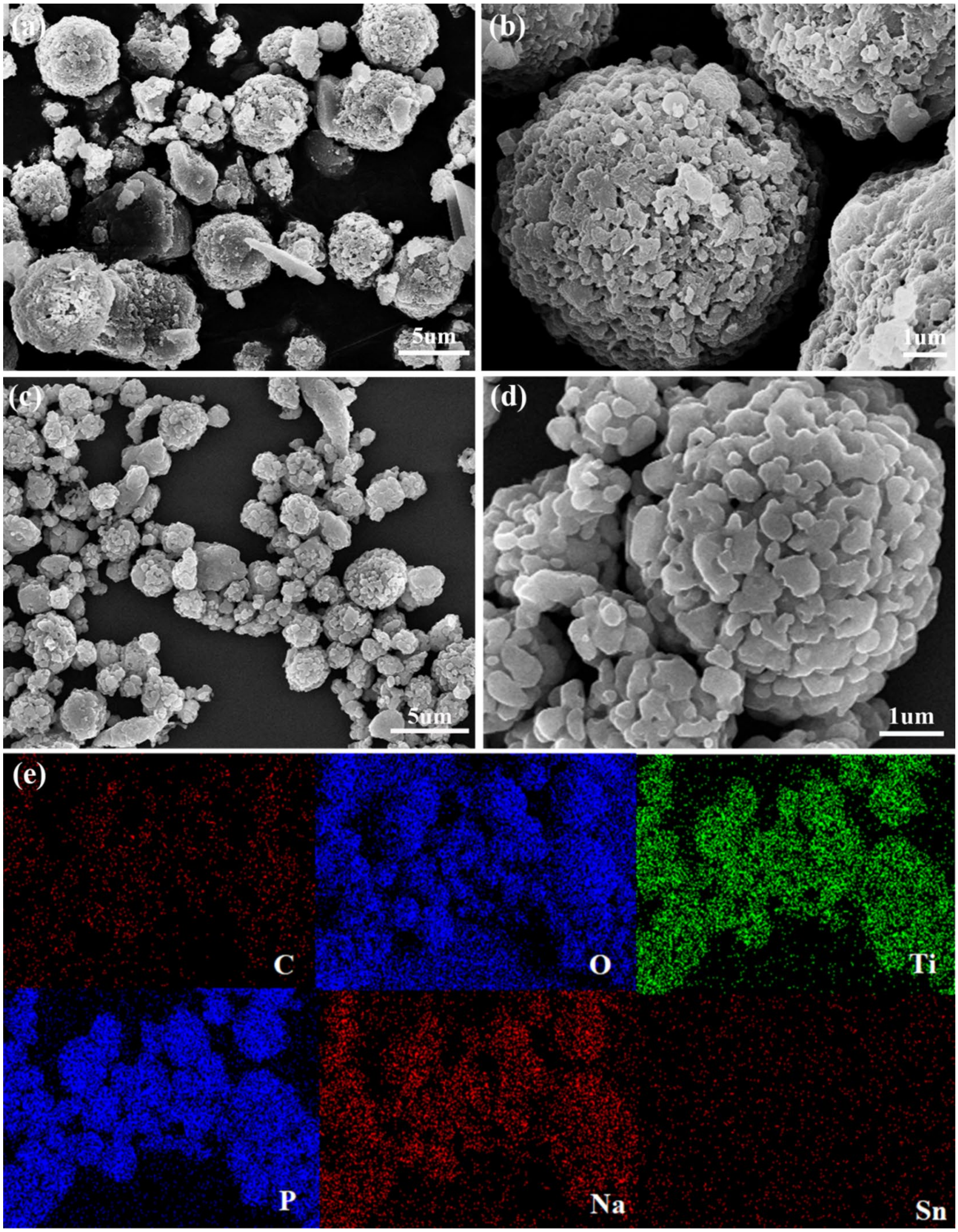

Fig. 2 **a**, **b** SEM images of $NaTi_2(PO_4)_3/C$, **c**, **d** SEM images of $NaSn_{0.02}Ti_{1.98}(PO_4)_3/C$, **e** EDS elemental Mappings of $NaSn_{0.02}Ti_{1.98}(PO_4)_3/C$

$NaSn_{0.02}Ti_{1.98}(PO_4)_3/C$ is approximately 91 Ω, significantly lower than that of $NaTi_2(PO_4)_3/C$ (173 Ω) and $NaTi_2(PO_4)_3$ (305 Ω). The decreased resistance of $NaSn_{0.02}Ti_{1.98}(PO_4)_3/C$ contributes to its improved electrochemical performance.

In order to better verify the promotion of Sn doping on the electrochemical reaction kinetics of the material, the sodium ion diffusion rate of the material was tested by the GITT method using LANDdt. The GITT curves and Na^+ diffusion coefficients for $NaTi_2(PO_4)_3/C$ and $NaSn_{0.02}Ti_{1.98}(PO_4)_3/C$ are shown in Fig. 4e, f. The Na^+ diffusion coefficient (D_{Na+}) of the electrode can be calculated from GITT data using Eq. (1):

$$DNa = \frac{4}{\pi\tau}(\frac{mBVm}{MBA})^2(\frac{\Delta ES}{\Delta E\tau})^2 \quad (1)$$

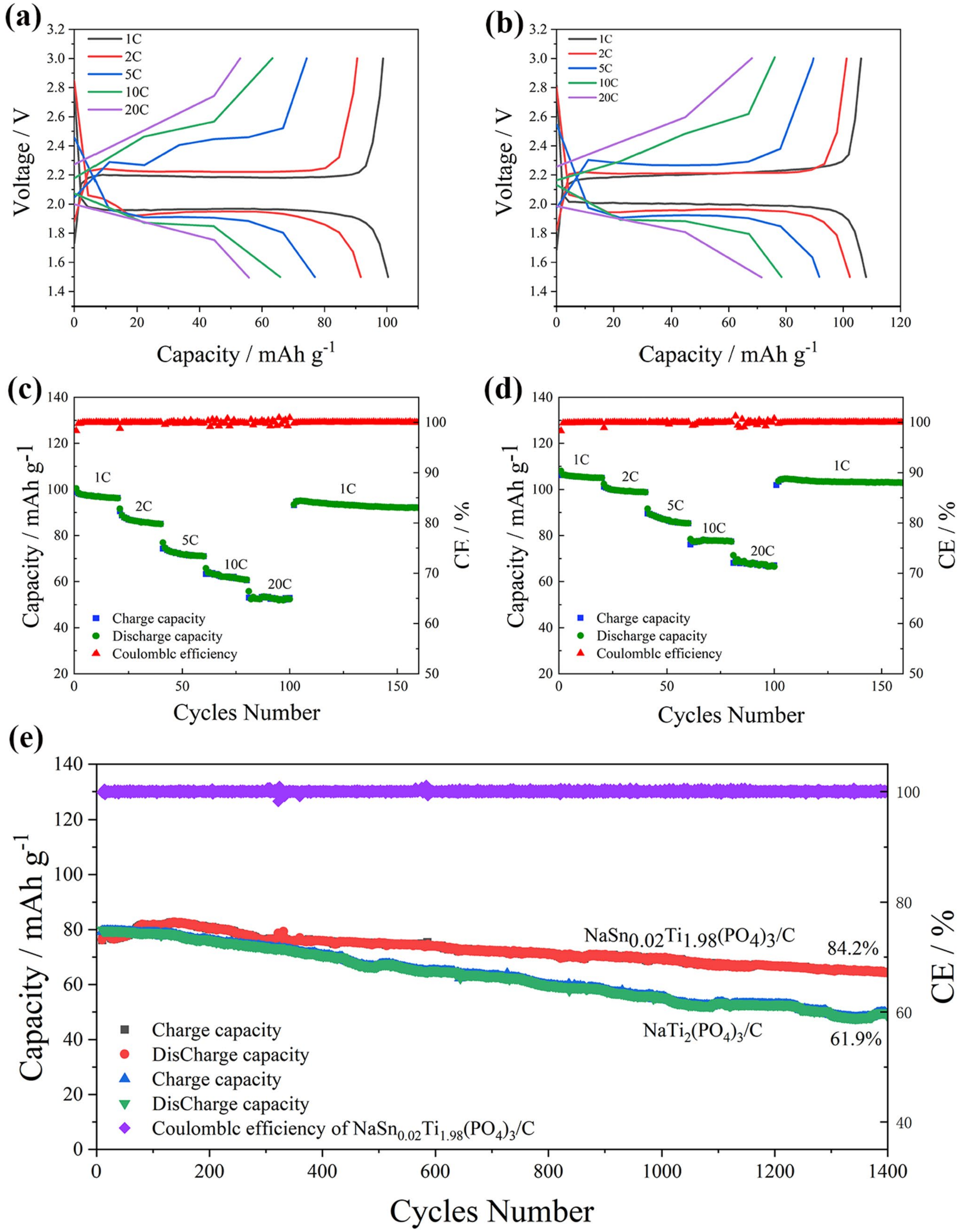
(a)
(b)
Voltage / V
Capacity / mAh g-1
1C
2C
5C
10C
20C
(c)
(d)
Capacity / mAh g-1
CE / %
Cycles Number
Charge capacity
Discharge capacity
Coulombic efficiency
(e)
NaSn0.02Ti1.98(PO4)3/C
84.2%
NaTi2(PO4)3/C
61.9%
Charge capacity
DisCharge capacity
Coulombic efficiency of NaSn0.02Ti1.98(PO4)3/C

◂**Fig. 3** **a** Discharge/charge curves of $NaTi_2(PO_4)_3/C$ at different rates, **b** discharge/charge curves of $NaSn_{0.02}Ti_{1.98}(PO_4)_3/C$ at different rates, **c** rate performance of $NaTi_2(PO_4)_3/C$ at different rates, **d** rate performance of $NaSn_{0.02}Ti_{1.98}(PO_4)_3/C$ at different rates, **e** long-term cycling performance of $NaTi_2(PO_4)_3/C$ and $NaSn_{0.02}Ti_{1.98}(PO_4)_3/C$ at 10C

In the equation, M_B and m_B are the molar mass and the active mass of $NaTi_2(PO_4)_3/C$ and $NaSn_{0.02}Ti_{1.98}(PO_4)_3/C$ electrode (1.96 mg/cm^2), V_m is the molar volume of $NaTi_2(PO_4)_3$, A is the surface area of the electrode piece (1.13 cm^2), τ is the interval time, ΔE_s is the voltage change of steady-state after a discharge pulse and open circuit standing, and ΔE_τ is the cell voltage change during a discharge pulse process. According to the Na^+ diffusion coefficient calculated from the GITT curve, the average value of D_{Na+} in the discharge process of $NaTi_2(PO_4)_3/C$ electrode is about 10^{-11}cm^2 s^{-1}, and the average value of D_{Na+} in the charging process is about 10^{-10}cm^2 s^{-1}. The average value of D_{Na+} in the discharge process of $NaSn_{0.02}Ti_{1.98}(PO_4)_3/C$ electrode is about 10^{-10}cm^2 s^{-1}, and the average value of D_{Na+} in the

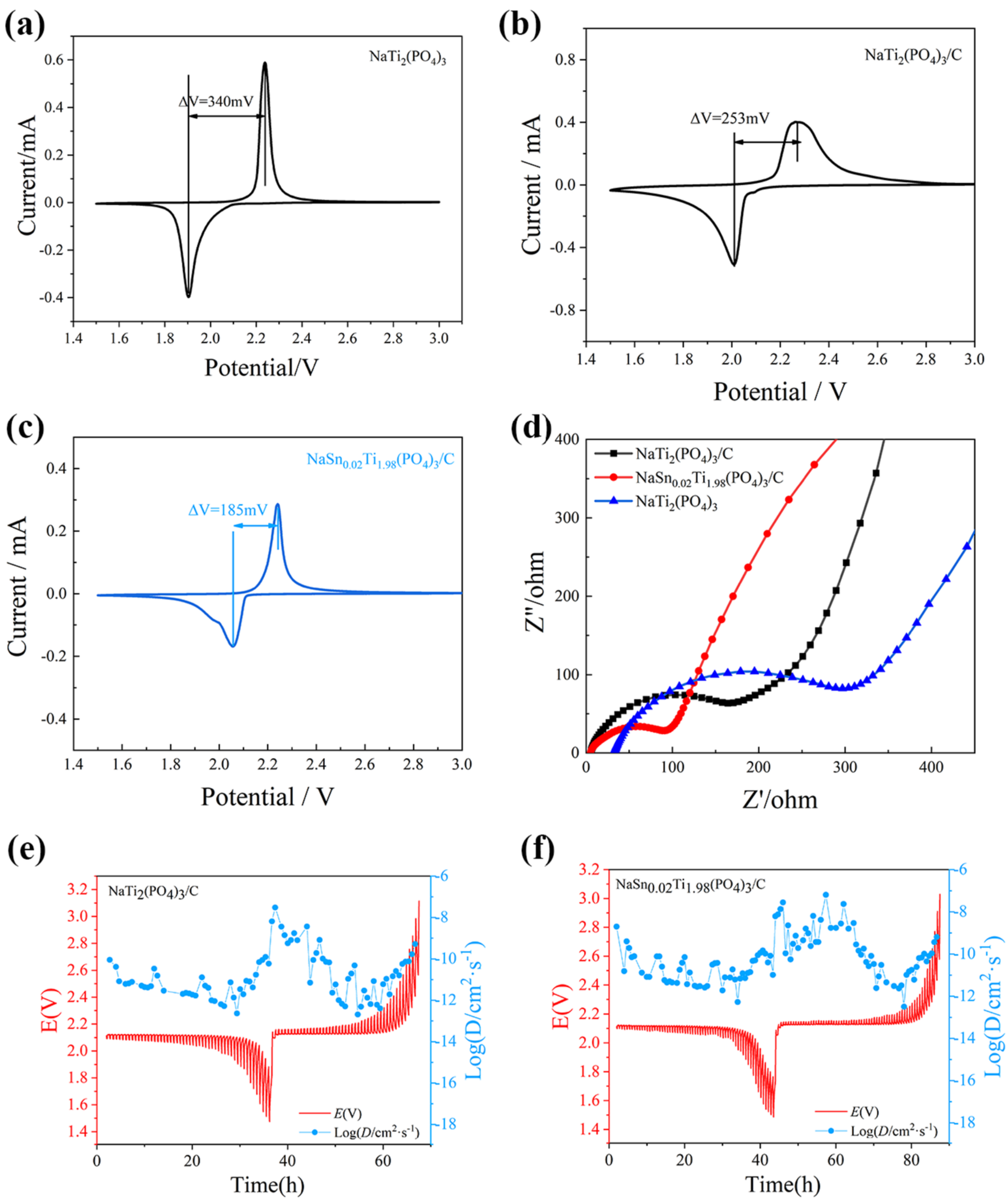

Fig. 4 **a** CV curve of $NaTi_2(PO_4)_3$ at 0.1 mV/s, **b** CV curve of $NaTi_2(PO_4)_3/C$ at 0.1 mV/s, **c** CV curve of $NaSn_{0.02}Ti_{1.98}(PO_4)_3/C$ at 0.1 mV/s, **d** Nyquist plots of $NaTi_2(PO_4)_3$, $NaTi_2(PO_4)_3/C$, $NaSn_{0.02}Ti_{1.98}(PO_4)_3/C$, **e** GITT curves and D_{Na+} of $NaTi_2(PO_4)_3/C$ charge/discharge process, **f** GITT curves and D_{Na+} of $NaSn_{0.02}Ti_{1.98}(PO_4)_3/C$ charge/discharge process

charging process is about $10^{-9}cm^2\ s^{-1}$. It can be seen that $NaSn_{0.02}Ti_{1.98}(PO_4)_3/C$ has a greater D_{Na+}. The sodium ion rate diffusion of $NaSn_{0.02}Ti_{1.98}(PO_4)_3/C$ is faster because of the substitution of Sn^{2+}, which enlarges the channel for Na^+ diffusion.

Conclusions

In summary, we prepared $NaSn_{0.02}Ti_{1.98}$ $(PO_4)3/C$ for organic SIBs to improve electrochemical performance. The doping of Sn^{4+} can increase the lattice spacing of the $NaTi_2(PO_4)_3$, thus accelerating the diffusion coefficient of Na^+. ICP analysis revealed that the mass percentage of Sn in $NaSn_{0.02}Ti_{1.98}(PO_4)_3/C$ is approximately 1.42%. The results of the TG test show that the carbon content of the sample is around 1.54%. The initial discharge-specific capacities of $NaSn_{0.02}Ti_{1.98}(PO_4)_3/C$ at 1C, 5C, 10C, and 20C rates are 108 mAh/g, 86 mAh/g, 76.3 mAh/g, and 71.4 mAh/g, respectively. After 1400 cycles at 10C, the capacity of the material decreases to 64.3 mAh/g, with a capacity retention rate of 84.2%. EIS results confirm that carbon coating leads to lower charge transfer impedance and increased ion diffusion coefficient in $NaTi_2(PO_4)_3$. Therefore, $NaSn_{0.02}Ti_{1.98}(PO_4)_3/C$ has better electrochemical performance and fast charge/discharge performance.

Funding This work was supported by the Natural Science Foundation of Jiangsu Province (Grants No. BK20201 472) and Changzhou Science and Technology Bureau (CM20223017).

Data availability The datasets generated during and/or analyzed the current study are available from the corresponding author on reasonable request.

Declarations

Conflict of interest The authors declare no competing interests.

References

1. Wang Z, Ni J, Li L (2022) Gradient designs for efficient sodium batteries. ACS Energy Lett 7(11):4106–4117
2. Shen X, Qian T, Chen P, Liu J, Wang M, Yan C (2018) Bioinspired polysulfiphobic artificial interphase layer on lithium metal anodes for lithium sulfur batteries. ACS Appl Mater Interfaces 10(36):30058–30064
3. Wang J, Wang Z, Ni J, Li L (2022) Electrospinning for flexible sodium-ion batteries. Energy Stor Mater 45:704–719
4. Liao W, Hung T, Abdelaal MM, Chao C, Fang C, Mohamed SG, Yang C (2022) Highly efficient sodium-ion capacitor enabled by mesoporous $NaTi_2(PO_4)_3/C$ anode and hydrogel-derived hierarchical porous activated carbon cathode. J Energy Storage 55:105719
5. Zheng W, Wu M, Yang C, Tang Z, Hu H (2020) Sn substitution endows $NaTi_2(PO_4)_3/C$ with remarkable sodium storage performances. Ceram Int 46(9):12921–12927
6. He H, Gan Y, Mu M, Yuan J, Zhang C, Zhang X, Li X, Ma X, Yu H, Mou J, Liu J (2023) Fabrication of nano-solid spherical Nb_2O_5/nitrogen-doped carbon composite for high-performance sodium-ion battery anodes. J Solid State Electrochem 27(9):2337–2345
7. Wu S, Bashir T, Zhang Y and Gao L (2023) Scalable single-step synthesis of α-Nb_2O_5@C@Ti_3C_2 composite as high power and long life anode material for sodium-ion batteries. J Solid State Electrochem
8. Yang C, Sun X, Zhang YR, Liu Y, Zhang QA, Yuan CZ (2019) Facile synthesis of hierarchical $NaTi_2(PO_4)_3/Ti_3C_2$ nanocomposites with superior sodium storage performance. Mater Lett 236:408–411
9. Liu R, Liu H, Sheng T, Zheng S, Zhong G, Zheng G, Liang Z, Ortiz G F, Zhao W, Mi J, Yang Y (2018) Novel 3.9 V Layered $Na_3V_3(PO_4)_4$ Cathode material for sodium ion batteries. ACS Appl Energy
10. Kitajou A, Yamashita M, Kobayashi W, Okada M, Nanami T, Muto S (2022) Anode properties of $NaTi_2(PO_4)_3$ prepared by adding excess Na_2CO_3 for aqueous sodium-ion batteries. ACS Appl Energy Mater 1(8):3603–3606
11. Xu T, Zhao M, Li Z, Su Z, Ren W, Yang S, Pol VG (2022) A high rate and long cycling performance $NaTi_2(PO_4)_3$ core–shell porous nanosphere anode for aqueous sodium-ion batteries. Energy Technol-ger 10(11):2200970
12. Wei P, Liu Y, Su Y, Miao L, Huang Y, Liu Y, Qiu Y, Li Y, Zhang X, Xu Y, Sun X, Fang C, Li Q, Han J, Huang Y (2019) F-Doped $NaTi_2(PO_4)_3/C$ Nanocomposite as a high-performance anode for sodium-ion batteries. ACS Appl Mater Interfaces 11(3):3116–3124
13. Lei P, Li S, Luo D, Huang Y, Tian G, Xiang X (2019) Fabricating a carbon-encapsulated $NaTi_2(PO_4)_3$ framework as a robust anode material for aqueous sodium-ion batteries. J Electroanal Chem 847:113180
14. Wu J, Yang L, Liu H, Bu H, Wang W, Zeng C, Zhu S (2022) Effect of Al doping on electrochemical performance of $NaTi_2(PO_4)_3/C$ anode for aqueous sodium ion battery. J Appl Electrochem 52(11):1563–1572
15. Kavitha KR, Babu BM, Vadivel S, Shkir M, Hakami J, Minnam Reddy VR (2022) Promoting the performances of $NaTi_2(PO_4)_3$@C porous composite as novel anode materials for application in sodium ion battery. Ceram Int 48(19, Part B):29514–29522
16. Cao X, Yang Y (2018) Facile synthesis of $NaTi_2(PO_4)_3$-carbon composite through solid state method and its application in aqueous sodium ion battery. Mater Lett 231:183–186
17. Nian Z, Zhang J, Du Y, Jiang Z, Chen Z, Li Y, Han C, He Z, Meng W, Dai L, Wang L (2021) Chlorine doping enables $NaTi_2(PO_4)_3/C$ excellent lithium ion storage performance in aqueous lithium ion batteries. J Electroanal Chem 880:114941
18. Jiang Z, Li Y, Han C, Huang Z, Wu X, He Z, Meng W, Dai L, Wang L (2020) Raising Lithium Storage Performances of $NaTi_2(PO_4)_3$ by Nitrogen and Sulfur Dual-Doped Carbon Layer. J Electrochem Soc 167(2):020550
19. Mao W, Zhang S, Cao F, Pan J, Ding Y, Ma C, Li M, Hou Z, Bao K, Qian Y (2020) Synthesis of $NaTi_2(PO_4)_3$@C microspheres by an in situ process and their electrochemical properties. J Alloy Compd 842:155300
20. Zhang L, Zhou Y, Li Y, Ma W, Wu P, Zhu X, Wei S, Zhou Y (2022) Achieving in-situ hybridization of $NaTi_2(PO_4)_3$ and N-doped carbon through a one-pot solid state reaction for high performance sodium-ion batteries. J Solid State Chem 310:123036
21. Yan H, Zhang B, Fu Y, Wang Y, Dong J, Li Y, Li Z (2022) Gd^{3+}-doped $NaTi_2(PO_4)_3$@C negative material with superior

Na-storage property for sodium-ion batteries. J Alloy Compd 892:162068
22. He X, Zou Q, Wu L (2021) Zr doping and carbon coating endow $NaTi_2(PO_4)_3$ electrode with enhanced performances. J Alloy Compd 859:157836
23. Qu D, Chen Z, Xu G, Liu X, Wei X, Yang L (2020) Mesoporous Mn-doped and carbon-coated $NaTi_2(PO_4)_3$ nanocrystals as an anode material for improved performance of sodium-ion hybrid capacitors. J Mater Sci-Mater El 31(20):17550–17562
24. Voronina N, Jo JH, Choi JU, Jo CH, Kim J, Myung ST (2019) Nb-Doped titanium phosphate for sodium storage: electrochemical performance and structural insights. J Mater Chem A 7(10):5748–5759
25. Yu ZE, Lyu YC, Zou ZY, Su N, He B, Wang SF, Shi SQ, Guo BK (2021) Understanding the structural evolution and storage mechanism of NASICON-structure $Mg_{0.5}Ti_2(PO_4)_3$ for Li-ion and Na-ion batteries. ACS Sustain Chem Eng 9(40):13414–13423
26. Zhao Y, Wei Z, Pang Q, Wei Y, Cai Y, Fu Q, Du F, Sarapulova A, Ehrenberg H, Liu B, Chen G (2017) NASICON-Type $Mg_{0.5}Ti_2(PO_4)_3$ Negative electrode material exhibits different electrochemical energy storage mechanisms in Na-Ion and Li-ion batteries. ACS Appl Mater Interfaces 9(5):4709–4718
27. Difi S, Saadoune I, Sougrati MT, Hakkou R, Edstrom K, Lippens PE (2015) Mechanisms and performances of $Na_{1.5}Fe_{0.5}Ti_{1.5}(PO_4)_3$/C composite as electrode material for Na-ion batteries. J Phys Chem C 119(45):25220–25234
28. Wang QY, Luo YX, Gu FP, Shui M, Shu J (2020) The preparation, characterization, electro-chemical performance and transporting mechanism of $Na_{1.25}Cr_{0.25}Ti_{1.75}(PO_4)_3$/C as anode material for SIBs. Solid State Ion 352
29. Zhao Y, Zhang P, Liang J, Xia X, Ren L, Song L, Liu W, Sun X (2022) Uncovering sulfur doping effect in MnO_2 nanosheets as an efficient cathode for aqueous zinc ion battery. Energy Stor Mater 47:424–433
30. Deng S, Zhu H, Liu B, Yang L, Wang X, Shen S, Zhang Y, Wang J, Ai C, Ren Y, Liu Q, Lin S, Lu Y, Pan G, Wu J, Xia X, Tu J (2020) Synergy of ion doping and spiral array architecture on $Ti_2Nb_{10}O_{29}$: a new way to achieve high-power electrodes. Adv Funct Mater 30(25):2002665

Publisher's Note Springer Nature remains neutral with regard to jurisdictional claims in published maps and institutional affiliations.

Springer Nature or its licensor (e.g. a society or other partner) holds exclusive rights to this article under a publishing agreement with the author(s) or other rightsholder(s); author self-archiving of the accepted manuscript version of this article is solely governed by the terms of such publishing agreement and applicable law.